Procedia Engineering
Volume 143, 2016, Pages 556–565
Advances in Transportation Geotechnics 3 . The 3rd International Conference on Transportation Geotechnics (ICTG 2016)

Importance of Controlling the Degree of Saturation in Soil Compaction

Fumio Tatsuoka[1] and Antonio G. Correia[2]
[1]*Tokyo University of Science, Chiba, Japan*
[2]*University of Minho, Guimarães, Portugal*
Tatsuoka@rs.noda.tus.ac.jp, agc@civil.uminho.pt

Abstract
In the typical conventional fill compaction, the dry density ρ_d and the water content w are controlled in relation to $(\rho_d)_{max}$ and w_{opt} determined by laboratory compaction tests using a representative sample at a certain compaction energy level CEL. Although CEL and actual soil type affect significantly the values of $(\rho_d)_{max}$ and w_{opt}, they change inevitably in a given earthwork project while CEL in the field may not match the value used in the laboratory compaction tests. Compaction control based on the stiffness of compacted soil in the field has such a drawback that the stiffness drops upon wetting more largely as the degree of saturation, S_r, of compacted soil becomes lower than the optimum degree of saturation $(S_r)_{opt}$ defined as S_r when $(\rho_d)_{max}$ is obtained for a given CEL. In comparison, the value of $(S_r)_{opt}$ and the $\rho_d/(\rho_d)_{max}$ vs. S_r - $(S_r)_{opt}$ relation of compacted soil are rather insensitive to variations in CEL and soil type, while the strength and stiffness of unsoaked and soaked compacted soil is controlled by ρ_d and "S_r at the end of compaction". It is proposed to control not only w and ρ_d but also S_r so that S_r becomes $(S_r)_{opt}$ and ρ_d becomes large enough to ensue soil properties required in design.

Keywords: Degree of compaction, Degree of saturation, Dry density, Soil compaction, Water content

1 Introduction

In the typical conventional soil compaction procedure by end product specification, the dry density ρ_d and the water content w of compacted soil are controlled relative to the maximum dry density $(\rho_d)_{max}$ and the optimum water content w_{opt}, respectively, obtained by laboratory compaction tests performed on a representative sample at a certain compaction energy level (CEL), such as those of curve B-B shown in Fig. 1a (n.b., the test results described in Fig. 1a are explained in the next section). However, $(\rho_d)_{max}$ increases and w_{opt} decreases with an increase in CEL. In Fig. 1a, the compaction curve moves toward upper left with an increase in CEL associated with an increase in the number of passing (N) of a compaction machine in the full-scale compaction tests. The CEL in the top 10 cm-thick soil layer in the 30 cm-thick lift already exceeds Standard Proctor (1.0Ec) when N= 4, while the value when N= 16 is

Selection and peer-review under responsibility of the Scientific Programme Committee of ICTG 2016

doi:10.1016/j.proeng.2016.06.070

much higher than Modified Proctor (4.5Ec). Besides, when N= 16, the ρ_d values in the bottom 10 cm-thick soil layer (denoted as 16L) are much lower than those in the upper soil layer (denoted as N= 16), showing a fast decrease in CEL with depth. These facts indicate that, even at a nominally fixed CEL, actual CEL inevitably varies randomly associated with variations in actual N and actual lift and systematically with depth in each lift.

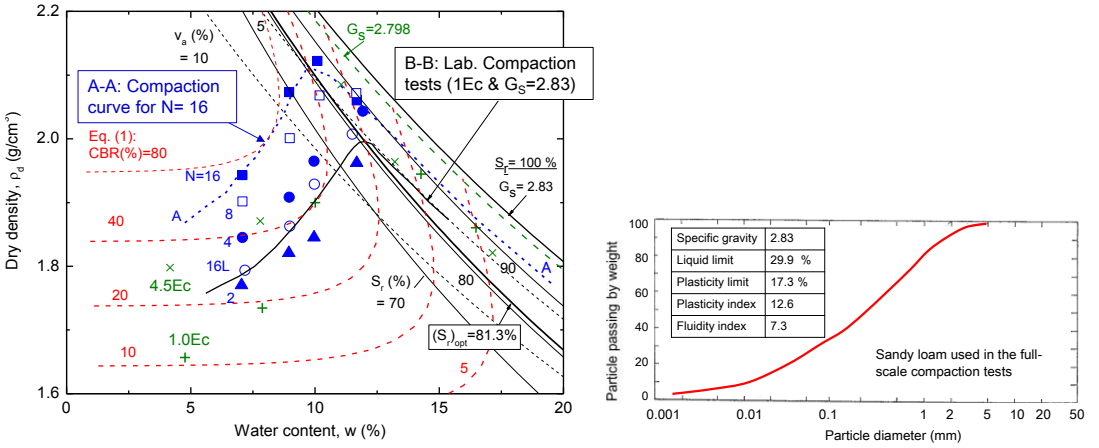

a) b)

Figure 1: a) Compaction characteristics with contours of unsoaked CBR from full-scale and laboratory compaction tests; and b) grading curve of sandy loam (after the data reported by Nemoto & Sasaki, 1994).

In this respect, Ishii et al. (1987) showed that CEL when compacting a 35 cm-thick soil layer by 16 passings of a flat surface 10 ton-vibratory steel roller, representative of typical modern fill compaction works, is approximately equivalent to 4.5Ec. In this case, the in-situ w_{opt} is much lower than "w_{opt} by laboratory compaction for 1.0Ec", while the in-situ $(\rho_d)_{max}$ becomes much higher than the value for 1.0Ec. Compaction at w > "w_{opt} for 1.0Ec" is often recommended in practice aiming at avoiding large collapse and a large decrease in the strength/stiffness upon wetting and/or obtaining the minimum saturated coefficient of hydraulic conductivity, k, for seepage-control soil structures. However, w higher than "w_{opt} for 1.0Ec" may become considerably higher than "in-situ w_{opt}", which may result in inefficient compaction and even over-compaction and/or a k value larger than the minimum.

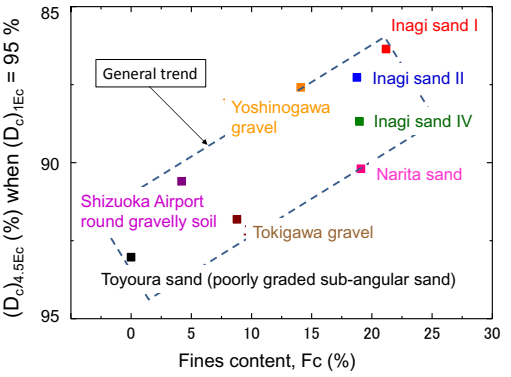

Figure 2: "D_c for 4.5Ec when D_c based on for 1.0Ec is equal to 95 %" vs. fines content relation of sandy & gravelly soils reported in Tatsuoka et al. (2015).

Besides, generally $(\rho_d)_{max}$ decreases and w_{opt} increases with an increase in fines content (FC) for otherwise similar grading characteristics (Tatsuoka, 2015). In Fig. 2, $(D_c)_{1.0Ec}$ denotes the ratio of ρ_d to $(\rho_d)_{max}$ obtained by compaction at 1.0Ec, while $(D_c)_{4.5Ec}$ denotes the ratio of ρ_d to $(\rho_d)_{max}$ obtained by compaction 4.5Ec. Both density indexes are used in the soil compaction control. In this figure, the value of $(D_c)_{4.5Ec}$ when $(D_c)_{1.0Ec}$= 95 % of sandy and gravelly soils is plotted against FC. The value of $(D_c)_{4.5Ec}$ becomes smaller than 95 % with an increase in FC and becomes about 85 % when FC= 30 %. Even when a fixed soil type is specified at a given site, actual soil type inevitably varies. The trend seen in Fig. 2 indicates that the value of $(\rho_d)_{max}$ for a fixed CEL inevitably varies in the field due to inevitable variations in the actual soil type. In summary, even if fixed CEL and soil type are specified in a given earthwork project, due to inevitable variations in the actual CEL and soil type, the in-situ compaction curve moves from time to time and from place to place. So, it is usually very hard to exactly capture current in-situ values of $(\rho_d)_{max}$ and w_{opt}.

As an alternative method, it has become popular to control soil compaction based on the stiffness of compacted soil frequently evaluated from the response acceleration of a compaction machine in operation or by 'portancemeter', as well as by dynamic loading plate tests, including the falling weight deflectometer test (Gomes Correia, 2008; Gomes Correia and Magnan, 2012). However, the strength/stiffness under saturated conditions is used in design of soil structures that may get wet or saturated by heavy/prolong rains, floods, impounding etc. during the long lifecycle span. Besides, the stiffness decreases by wetting differently depending on the value of S_r relative to the optimum degree of saturation $(S_r)_{opt}$ (defined as S_r at which $(\rho_d)_{max}$ is obtained for a given CEL of a given soil type). At the S_r= $(S_r)_{opt}$ state, the saturated strength/stiffness of a given soil type becomes nearly its maximum for a given CEL (as shown below). It is not possible to identify the S_r= $(S_r)_{opt}$ state only by measuring the stiffness of compacted soil under unknown unsaturated conditions.

In this paper, it is shown that the value of $(S_r)_{opt}$ and "the $\rho_d/(\rho_d)_{max}$ vs. S_r - $(S_r)_{opt}$ relation for a given CEL" of a given soil type are insensitive to variations in CEL and soil type. Besides, the CBR values before and after soaking, which are indexes of the strength and stiffness under unsoaked and soaked conditions, can be represented by different functions of ρ_d and "S_r at the end of compaction", not including CEL as a variable. Based on these findings, a new unified framework for fill compaction is proposed that controls the S_r value of compacted soil to become $(S_r)_{opt}$ and the ρ_d value to become large enough to ensure the soil properties required in design of a given soil structure, together with pre-compaction control of the water content of fill material.

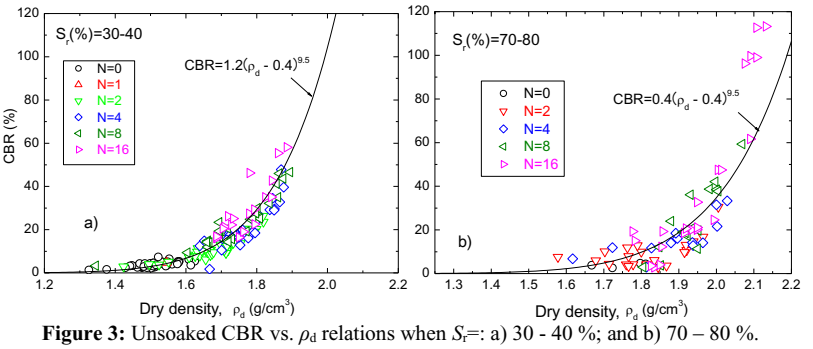

Figure 3: Unsoaked CBR vs. ρ_d relations when S_r=: a) 30 - 40 %; and b) 70 – 80 %.

Usually, the strength and stiffness of compacted soil is represented by a function of ρ_d and w. On the other hand, Fig. 3 shows the CBR - ρ_d relations when S_r= 30 - 40 % and 70 - 80 % obtained from all the full scale compaction tests. Similar results are obtained for other S_r values. It may be seen that the CBR vs. ρ_d relation for a fixed S_r is independent of compaction machine type and the number of passing N (i.e., independent of CEL). Accordingly, the test data were fitted by:

$$CBR = f_{CBR}(S_r) \cdot (\rho_d / \rho_w - b)^c \quad (1)$$

where ρ_w is the density of water; b= 0.4 and c= 0.9 (positive material constants); and f_{CBR} is a function of S_r at the end of compaction. In Fig. 4a, the values of f_{CBR} obtained from the relations shown in Fig. 3 and others are plotted against S_r. In Fig. 3, Eq. 1 fits the data very well. Importantly, the value of CBR for given values of ρ_d and S_r can be estimated by Eq. 1 without knowing CEL in the field, which is usually very difficult to know. It is to be noted that the value of S_r can be obtained from known values of ρ_d and w if the specific gravity of soil particles is known.

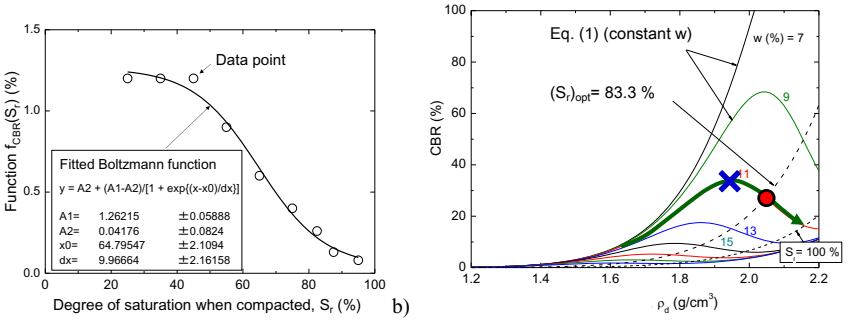

Figure 4: a) A function expressing the effects of S_r on unsoaked CBR; b) unsoaked CBR vs. ρ_d relations for different w values and for $(S_r)_{opt}$ and S_r= 100 % according to Eq. (1)

2 Full-Scale Compaction Tests

Fig. 1a shows typical results from a series of full-scale compaction tests using a wide variety of compaction machines performed in a large concrete pit (24 m-long, 3.5 m-wide and 1 m-deep) for a period from 1965 to 1990 (Nemoto & Sasaki, 1994). Overlying a 60 cm-thick base soil layer, a 30 cm-thick surface layer of sandy loam (Fig. 1b) was prepared repeatedly at different water contents for respective compaction machines. The machine types were those used in actual earthworks, including smooth wheel steel rollers and pneumatic rubber-tired rollers, both being either static or vibratory. In each test, after soil-spreading with preliminary compaction by eight passings of a light machine, a full-scale compaction test was performed. The ρ_d value of the top 10 cm-thick soil layer was measured four times by the sand-replacement method after the number of passing N= 0, 2, 4, 8 and 16. The ρ_d value of the bottom 10 cm-thick soil layer was measured only after N= 16. The data points ▲, ○, ●, □ and ■ denote the average values of ρ_d and w from a test series using a 1.6 ton-vibratory pneumatic tire roller. The CBR value was measured three times after respective N values. The broken curves are the contours of unsoaked CBR (explained below). The data points × and + denote the results of the laboratory compaction tests (1.0Ec & 4.5Ec) performed in 2012 at Tokyo University of Science. CBR as a Function of ρ_d and S_r

Fig. 4b shows the relationships between the unsoaked CBR and ρ_d for several w values and those for S_r= $(S_r)_{opt}$ and 100 % obtained from Eq. 1. The following trends may be seen. With an increase in ρ_d associated with an increase in CEL during compaction at a fixed w, the CBR value increases until CBR becomes the maximum at a point denoted by X, for example. At this point, S_r is still lower than $(S_r)_{opt}$, while the S_r= $(S_r)_{opt}$ state, where ρ_d= "$(\rho_d)_{max}$ for the transient value of CEL", is realized at a point denoted by a solid circle. This means that the S_r= $(S_r)_{opt}$ state (i.e., the $(\rho_d)_{max}$ state for a given CEL) cannot be detected only by measuring the values of CBR or the stiffness of compacted soil. In other words, as is empirically very well known, the maximum compaction efficiency is not necessarily achieved by maximizing the value of CBR or stiffness of compacted soil.

The contours of unsoaked CBR obtained from Eq. 1 are depicted in Figs. 1a and 5a. On the other hand, the soaked CBR is a relevant index of the strength and stiffness of saturated soil and usually used in the design of soil structures that would get wet or saturated by heavy/prolonged rains, floods, impounding etc. during their lifecycle span (Tatsuoka et al., 2014). In Fig. 5a, in addition to the contours of unsoaked CBR, those of CBR after soaking are depicted. The values of soaked CBR were obtained by incorporating the effects of soaking into the function f_{CBR} in Eq. 1. The soaking effects were evaluated by a series of laboratory CBR tests performed on unsoaked and soaked samples compacted to various ρ_d and S_r states using the same soil type as used in the full-scale compaction tests (Tatsuoka, 2015). Tatsuoka (2011 & 2015) showed that these soaked CBR values and the drained strength and stiffness of saturated specimens of a number of well-graded sandy and gravelly soils evaluated by drained triaxial compression (TC) tests are also a function of ρ_d and "S_r at the end of compaction". These facts indicate that "w during compaction" is not the basic controlling parameter among others for the stress-strain properties of soil. For this reason, the shape of the CBR contours depicted on the ρ_d and w plane is very complicated (Figs. 1a & 6a): in particular, each contour under the soaked or unsoaked condition crosses a vertical constant w line two times for w in some range.

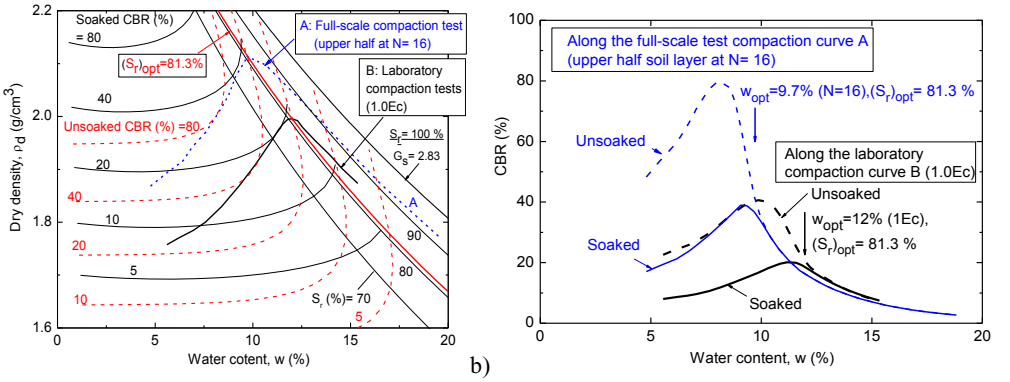

Figure 5: a) Contours of unsoaked & soaked CBR depicted on the ρ_d - w plane; and b) CBR – w relations along two compaction curves, A and B, shown in Fig. 5a.

In Fig. 5a, curve A is the compaction curve fitted to the data points when N= 16 in the full-scale compaction test depicted referring to compaction curve B obtained by laboratory compaction tests (1.0Ec). Fig. 5b shows the relationships between the unsoaked and soaked values of CBR and "w during compaction" when moving along compaction curves A and B. In both cases, when compacted to $S_r < (S_r)_{opt}$, the unsoaked CBR is relatively high, whereas it drops largely upon soaking. Collapse deformation upon wetting is also significant if ρ_d is low (Tatsuoka & Shibuya, 2014). When $S_r = (S_r)_{opt}$, irrespective of CEL, CBR drops only slightly upon soaking, while the soaked CBR is close to its maximum along compaction curve A or B. Besides, collapse deformation upon wetting is insignificant, in particular when well compacted (Tatsuoka & Shibuya, 2014). When $S_r > (S_r)_{opt}$, the drop of CBR upon soaking is negligible, whereas CBR is low and becomes lower with an increase in w along compaction curve A or B. These results indicate that the $S_r = (S_r)_{opt}$ state, which can be reached without knowing in-situ CEL, is the relevant compaction target irrespective of CEL.

2.1 Unified Compaction Curve

In Fig. 6a, the data presented in Fig. 1a have been re-plotted changing the abscissa from w to S_r while adding other laboratory compaction test data of the same soil type. In this figure, the compaction curves from the laboratory and full-scale compaction tests at different CELs exhibit nearly the same shape and nearly the same $(S_r)_{opt}$ value (81.3 % on average). Then, the $\rho_d/(\rho_d)_{max}$ vs. "S_r - $(S_r)_{opt}$" relations obtained

under the different compaction conditions have become nearly the same (Fig. 7b). Joslin (1959) reported 26 average compaction curves derived from 10,000 laboratory compaction curves for 1.0Ec on a very large range of soil types (Fig. 7a). Fig. 7b shows the $\rho_d/(\rho_d)_{max}$ vs. S_r - $(S_r)_{opt}$ relations obtained from these 26 curves by using the $(S_r)_{opt}$ value of the respective curves. In Fig. 7b, the all relations are very similar without showing a specific trend of scatter according to soil type. Besides, the relations presented in Figs. 6b and 7b are very similar to each other.

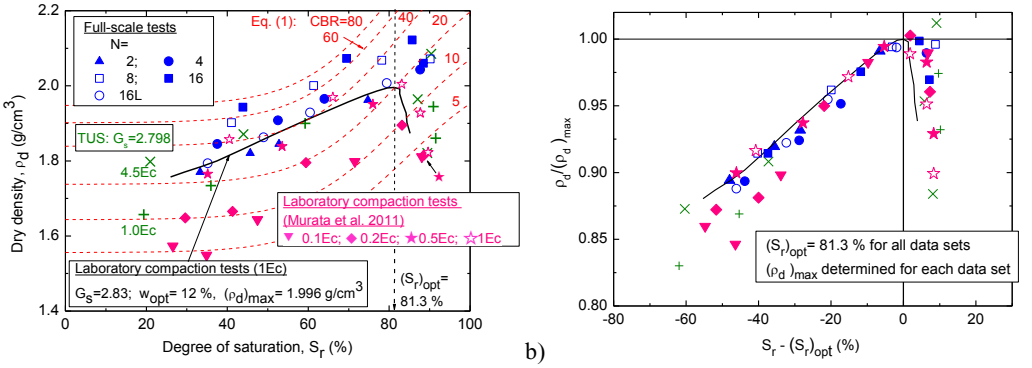

Figure 6: a) Compaction curves and CBR contours on ρ_d - S_r plane of the data presented in Fig. 1a; and b) $\rho_d/(\rho_d)_{max}$ vs. "S_r - $(S_r)_{opt}$" relations.

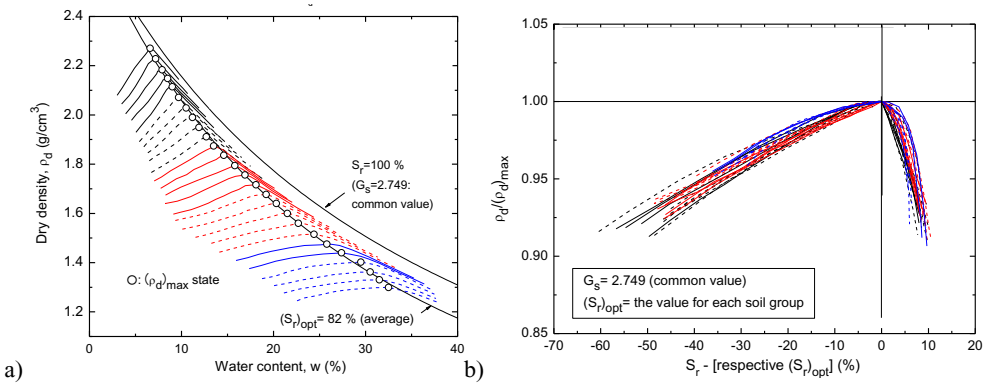

Figure 7: Compaction test data for 1.0Ec by Ohio State (Joslin, 1959): a) 26 average $\rho_d - w$ relations; and b) $\rho_d/(\rho_d)_{max}$ vs. $S_r - (S_r)_{opt}$ relations.

Fig. 8 shows the $(S_r)_{opt}$ vs. $(\rho_d)_{max}$ relations obtained from laboratory compaction tests of a very wide range of soil type, from clayey soil to well-graded gravelly soil. With the whole data, the scatter of $(S_r)_{opt}$ is not small. The cause for this scatter is not known. Yet, in this extreme large range of $(\rho_d)_{max}$, there is no specific effect of $(\rho_d)_{max}$ on the $(S_r)_{opt}$ value. Two broken curves denote the S_r - ρ_d relations for constant air void ratios, v_a. Along these relations, the S_r value decreases with an increase in $(\rho_d)_{max}$. This means that the value of v_a where $(\rho_d)_{max}$ is obtained for a fixed CEL, $(v_a)_{opt}$, is not constant for a wide range of $(\rho_d)_{max}$.

All the compaction test data of a wide range of soil type from soft clay to well-graded gravelly soil performed at a wide range of CEL that are available to the authors, including those shown in this paper, show that the $\rho_d/(\rho_d)_{max}$ vs. S_r - $(S_r)_{opt}$ relation and the value of $(S_r)_{opt}$ are insensitive to changes in CEL and soil type (Tatsuoka, 2015). Then, we can reasonably assume that these quantities are kept essentially constant in a given earthwork project in which fixed soil type and CEL are specified. Then, for any combination of actual CEL and soil type, with a known value of $(S_r)_{opt}$, the true degree of compaction

$(D_c)_t$ at given moment and location is readily obtained by substituting a measured in-situ S_r into the $(D_c)_t = \rho_d/(\rho_d)_{max}$ vs. S_r - $(S_r)_{opt}$ relation (Fig. 9a). If the field CEL is controlled to be nearly constant, the field $(D_c)_t$ value estimated as shown in Fig. 9a becomes a good density index defined for a fixed CEL, which is then a good index of the strength and stiffness of compacted soil. If both field values of ρ_d and S_r are available, the field ρ_d vs. S_r - $(S_r)_{opt}$ relation, thus the field ρ_d vs. w relation together with the $(\rho_d)_{max}$ value can be readily inferred (Fig. 9b).

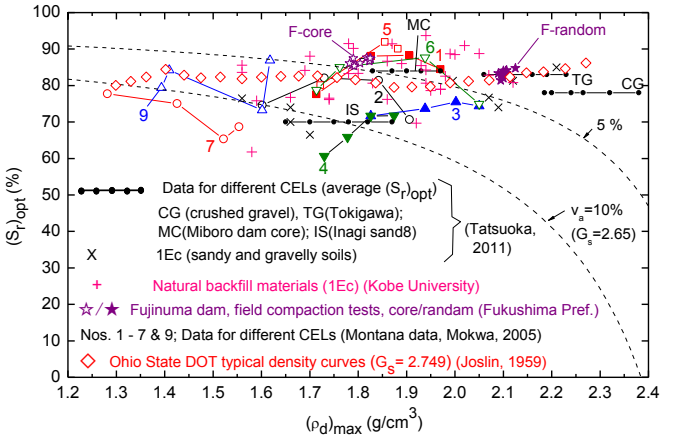

Figure 8: $(S_r)_{opt}$ - $(\rho_d)_{max}$ relations from a wide variety of laboratory compaction test data (Tatsuoka, 2015).

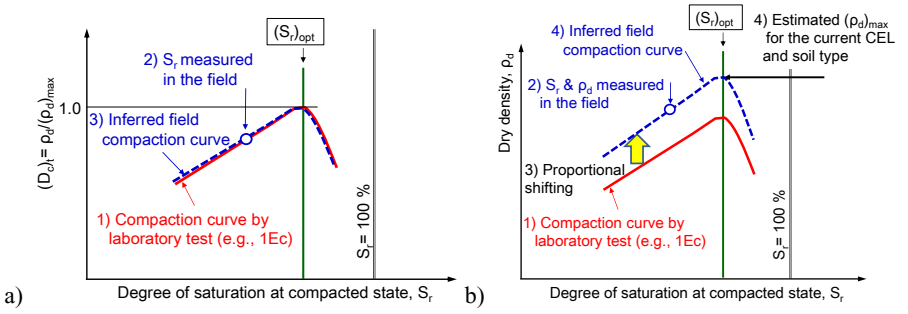

Figure 9: Inference of: a) $(D_c)_t = \rho_d/(\rho_d)_{max}$ - S_r relation; and b) ρ_d - S_r relation in the field.

3 Control of ρ_d, w and S_r

Based on the facts described above and others, the following framework is proposed for efficient and effective soil compaction control (Tatsuoka, 2015). Firstly, the target value of S_r is specified to be equal to the $(S_r)_{opt}$ value determined by laboratory compaction tests using a representative sample at a relevant CEL which is as much as representative of the field value. This process is the same as performed for the conventional soil compaction control. Secondly, the target value of ρ_d is determined in such that soil properties considered in the design of a given soil structure can be realized. In this respect, Figs. 10a, b and c schematically illustrate the contours on the $\rho_d - w$ plane showing the control boundary conditions for three typical soil properties that are often considered in design. The dotted zones indicate the corresponding acceptable or allowable zones. These contours and zones were depicted based on the experimental results presented in Fig. 1a and others (Tatsuoka & Shibuya, 2014; Tatsuoka 2015). Thirdly, the four major actions that result in poor soil compaction are: 1) too low water content and 2)

too high water content of the fill material; 3) too low CEL resulting from the use of a too light compaction machine with a too small number of passing and a too large lift; and 4) the use of less compactable soil type. So, to restrain these actions while allowing inevitable but limited variations in w, ρ_d and S_r, the control boundaries for these quantities are introduced, as listed in the table inset in Fig. 10. The target compaction state should be located inside all of such acceptable zones for required soil properties, as shown in Fig. 10a, b, and c.

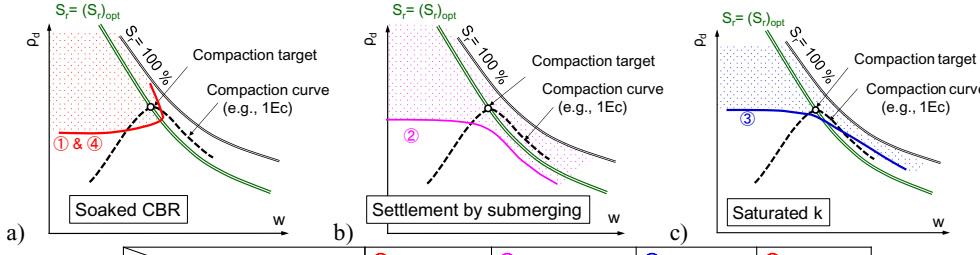

Control boundaries \ Required properties of compacted soil		① High strength & stiffness	② Small collapse, & ②' small strength reduction upon wetting	③ Low permeability	④ No danger of over-compaction
For fill material to be compacted	WL for w	Important[1)]	**Essential**	Important	
	WU for w	**Essential**[2)]			**Essential**
For compacted fill	DL for D_c	**Essential**	Important	Important	Important
	SL for S_r		**Essential**	**Essential**	
	SU for S_r	Important			**Essential**

Notes 1) & 2): These control boundaries are either essential or important to achieve this soil property.

Figure 10: a) – c) Contours of allowable bounds of three typical soil properties often required in design and the corresponding acceptable or allowable zones.

Fig. 11a summarizes the overall picture of the soil compaction control proposed based on the analysis shown above. This method does not contradict the conventional control procedures but it unifies them into a single consistent framework comprising steps 1 – 9 depicted in Fig. 11a and explained below.

Step 1: Compaction target T is determined, where $S_r = (S_r)_{opt}$ (irrespective of CEL); and $\rho_d = (\rho_d)_{target}$.

Step 2: The in-situ target compaction curve that passes point T is obtained as shown in Fig. 9b.

Step 3: The allowable lower bound for ρ_d, denoted as DL, is determined, where $D_c = \rho_d/(\rho_d)_{target}$ x 100 % is equal to a specified value, such as 95 %. One of the rationales for 95 % is presented in Fig. 12. Fig. 12 shows the distributions of 19,245 data of D_c from 94 highway embankment construction projects for a period from November 2004 to June 2008. In these projects, 200 kN-level vibratory steel rollers (flat surface) were used and the fill materials had $D_{max} \leq 40$ mm and $FC \leq 20$ %. For each CEL (1.0Ec or 4.5Ec), the average of all measured D_c values is larger by about 5 - 6 % than the allowable lower bound. The purposes of setting DL and the others are listed in the table inset in Fig. 10.

Step 4: Point B where w= "the value at target T, w_{target}" is obtained along DL.

Step 5: The constant S_r curve that passes point B is defined as the allowable lower bound for S_r, SL. SL crosses the target compaction curve at point C. If the allowable lower bound of S_r is specified to satisfy requirements for hydraulic conductivity as depicted in Fig. 11c, for example, and if this S_r value is higher than the value at point B, the S_r value for SL (i.e., the S_r value at point C) is reset to be equal to that S_r value. Referring to Fig. 11b, suppose that, in a given earthwork project, the value of CEL is always kept rather constant while close to the one for the target compaction curve (CEL_T). This condition is becoming more likely in recent well-controlled earthworks. Suppose that the current compacted state is X, where $S_r > (S_r)_{SL}$. The deviation of state X from the target compaction curve is due to that the actual soil type for point X is less compactable than the one for which the target compaction curve has been determined. The true degree of compaction, $(D_c)_t$, for CEL_T at state X is defined as "ρ_d at point X"/"ρ_d

at point Y= $(\rho_d)_{max}$ for CEL_T of the actual soil type for point X". Then, even if state X is located much below the target point T while close to DL, as far as $S_r > (S_r)_{SL}$, the $(D_c)_t$ value for CEL_T at state X is higher than the apparent D_c at state C (= "ρ_d at point C"/$(\rho_d)_{target}$), so could be much higher than the allowable lower bound of D_c (typically 95 %). If the S_r value at state X is equal to $(S_r)_{opt}$, the $(D_c)_t$ value for CEL_T at state X is 100 %. This is one of the benefits of maintaining the field CEL constant that can be obtained by controlling S_r to be close to $(S_r)_{opt}$.

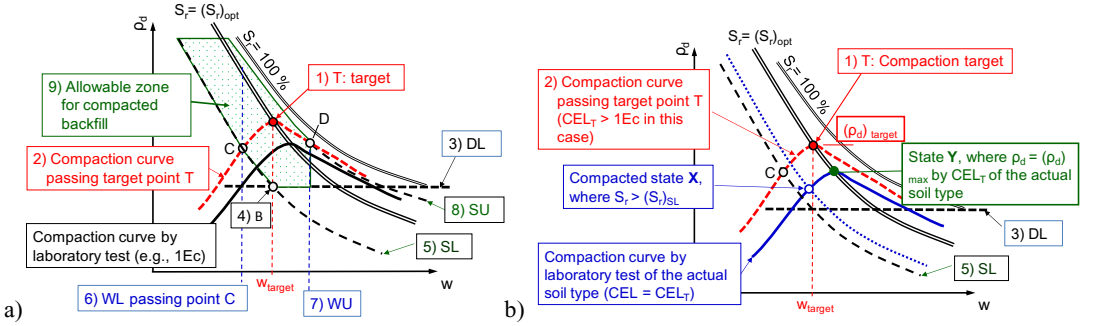

Figure 11: a) Soil compaction control to achieve the soil properties required in design of a given soil structure; and b) the true degree of compaction $(D_c)_t$ when CEL is well controlled to be constant equal to CEL_T.

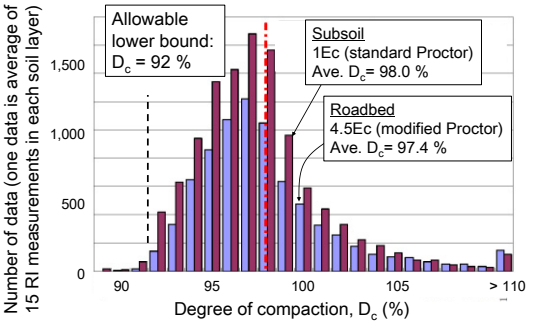

Figure 12: Distributions of measured values of D_c of sandy and gravelly soils for highway embankments (Yokota & Nakamura 2009).

Step 6: The allowable lower bound for w, WL, is specified to pass point C: i.e., w_{WL}= "w at point C".

Step 7: The allowable upper bound for w, WU, where $w = w_{WU} = w_{target} + x$, is specified to avoid too low strength/stiffness and to prevent over-compaction. Trial field compaction tests may be necessary to obtain the reliable value of x in each project. Only the fill material having w between w_{WL} and w_{WU} is allowed to be compacted.

Step 8: The allowable upper bound for S_r, SU, is specified to pass point D, where WU crosses the target compaction curve. Alternatively, the allowable upper bound for S_r, SU, is firstly specified as $(S_r)_{opt}$ + 5 %, for example, then point D is obtained where SU crosses the target compaction curve. Then, WU is obtained to pass point D.

Step 9: The acceptable or allowable zone for compacted soil comprising boundaries SL, DL, WU and SU is specified. Basically, WL is not necessary to define this zone. This is because compacted soils with $w < w_{WL}$ can satisfy the required soil proprieties if the compacted state is located in this allowable zone. In actuality, if $w < w_{WL}$, it is very difficult to reach this allowable zone even by compaction using a very high CEL. So, compaction using backfill having $w < w_{WL}$ is not allowed. On the other hand, if the compacted fill is required to be homogeneous to prevent differential deformation, the left part of the allowable zone may be truncated by WL, and/or an upper bound for ρ_d, DU, may be additionally specified.

4 Conclusions

The optimum degree of saturation $(S_r)_{opt}$ is defined as S_r where $(\rho_d)_{max}$ is obtained for a given compaction energy level (CEL) and a given soil type. In this paper, it is shown that the value of $(S_r)_{opt}$ and the relationship between the true degree of compaction $(D_c)_t = \rho_d/(\rho_d)_{max}$ and $S_r - (S_r)_{opt}$ of compacted soil are rather insensitive to variations in CEL and soil type. Besides, the strength and stiffness before and after soaking are a function of ρ_d and "S_r at the end of compaction". Then, irrespective of in-situ CEL and soil type, which inevitably vary thus are usually unknown, the value of $(D_c)_t$ and the strength/stiffness of compacted soil at a given moment at a given location can be estimated from measured ρ_d and S_r. These empirical rules imply a strong correlation between S_r and suction. Therefore, these empirical relations should have very important implications in future developments in the non-saturated soil mechanics approach of mechanical related properties.

Based on the above, for relevant soil compaction control, it is proposed to examine whether S_r of compacted soil is close to $(S_r)_{opt}$ and ρ_d is large enough to achieve soil properties required in design, together with pre-compaction control of water content of fill material. By combining this proposed compaction control approach with frequent checking of the stiffness of compacted soil during and after compaction, the soil compaction control becomes quite efficient and effective.

References

Gomes Correia, A. (2008). Innovations in design and construction of granular pavements and railways. Advances in Transportation Geotechnics: Proc. of the 1st International Conference on Transportation Geotechnics (Eds: Ellis, E., Yu, Hai-Sui, McDowell, G., Dawson, A.R. & Thom, N.), 1-13. CRC Press, London, UK.

Gomes Correia, A. & Magnan, J-P. (2012). Trends and challenges in earthworks for transportation infrastructures. Advances in Transportation Geotechnics 2 (Eds: Miura, S., Ishikawa, T., Yoshida, N., Hisari, Y. & Abe, N.), 1-12. CRC Press, London, UK.

Ishii, T., Mishima, N. and Takashina, K. (1987). Characteristics of soil compaction using vibratory rollers and pneumatic-tire rollers, *Proc. 22th Annual Geotechnical Conference, JGS*, Niigata, 1683-1684 (in Japanese).

Murata, T., Tateyama, K., Yamamoto, T., Yoshida, T. and Kawano, K. (2011). Experimental method of predicting the compaction effect in fill work practice, *Geotechnical Engineering Journal, JGS*, 5(4): 589-601 (in Japanese).

Nemoto, T. and Sasaki, T. (1994). Soil compaction characteristics, *Celebrating 30th Anniversary Volume, Construction Method & Machinery Research Institute*, 45-58 (in Japanese).

Tatsuoka, F. (2011). Laboratory stress-strain tests for the development of geotechnical theories and practice*, Bishop Lecture, Proc. 5th International Conference on Deformation Characteristics of Geomaterials*, Seoul, Korea, Sept., 3-50.

Tatsuoka, F. and Shibuya, S. (2014). Several issues in the compaction of residential embankments, *Monthly Journal, the Foundation Engineering & Equipment (Kisoko),* 42(9): 17-23 (in Japanese).

Tatsuoka, F., Koseki, J. and Kuwano, J. (2014). Natural disasters mitigation by using construction methods with geosynthetics (earthquakes), *Keynote Lecture*, *Proc. 10th Int. Conf. on Geosynthetics (10ICG)*, Berlin, September.

Tatsuoka, F. (2015). Compaction characteristics and physical properties of compacted soil controlled by the degree of saturation, Keynote Lecture, *Deformation characteristics of geomaterials*, *Proc. of 6th International Conference on Deformation Characteristics of Geomaterials, Buenos Aires,* pp. 40-78.

Yokota, S. and Nakamura, M. (2009). Design and control of fill compaction for highway embankments, *Monthly Journal Kiso-Ko*, July, 37(7), 47- 50 (in Japanese).